atmosphere

MDPI

Article

North Atlantic and Indian Ocean links with Iraq Climate

Jasim Al-Khalidi [1,2,*], Mihai Dima [1], Petru Vaideanu [1] and Sabina Stefan [1]

[1] Faculty of Physics, University of Bucharest, P.O. Box, MG-11, 077125 Bucharest-Magurele, Romania; mihai@dmn.ro (M.D.); vaideanu.petru@yahoo.com (P.V.); Sabina_stefan@yahoo.com (S.S.)

[2] Department of Physics, Faculty of Sciences, University of Diyala, 32 Diyala, Iraq

* Correspondence: jasim@student.fizica.unibuc.ro; Tel.: +40-737909240

Received: 30 September 2017; Accepted: 24 November 2017; Published: 26 November 2017

Abstract: We investigate the connections of the North Atlantic and Indian Ocean sectors with Iraq winter/summer temperature and precipitation. Canonical Correlation Analyses (CCAs) are performed in order to identify potential links between Iraq climate and the atmospheric circulation over these two regions. Regression maps of 200 hPa and 500 hPa geopotential height and sea level pressure fields on the time series derived through CCAs are constructed in order to infer the physical mechanisms connecting the North Atlantic and Indian Ocean regions with Iraq climate. The winter temperature in this country is linked with the North Atlantic Scandinavian pattern, whereas the winter precipitation is associated with the North Atlantic Oscillation. In the free atmosphere, the connection with Iraq temperature is provided by Rossby waves, while the winter precipitation is linked to a more zonal structure. At surface, the air advection is a relevant mechanism through which North Atlantic modes appear to affect Iraq climate.

Keywords: Iraq climate; Canonical Correlation Analysis; sea level pressure; geopotential height; Scandinavian mode; North Atlantic Oscillation; Indian Ocean; regression analysis

1. Introduction

Temperature and precipitation are key parameters for Iraq climate. It is therefore important to identify the large-scale atmospheric circulation patterns which connect them. Previous studies investigating the controls of the Middle East climate have been concentrated mainly on the influences of the dominant oceanic and atmospheric modes, like the Atlantic Multidecadal Oscillation (AMO), El-Niño Southern Oscillation (ENSO) and North Atlantic Oscillation (NAO), during the winter and spring months, with less attention on other modes.

NAO is the dominant atmospheric mode in the North Atlantic sector [1]. The negative (positive) NAO phase leads to relatively cold (warm) conditions in central and northern Europe and to relatively warm (cold) conditions over southern Europe and the Mediterranean [2]. NAO is also linked to North Atlantic decadal climate variability [3]. Most studies related to NAO are focused on the winter months because this is when the atmosphere is most active and turbulent [4]. The westerly winds associated with NAO bring low-pressure systems and moisture from the Mediterranean, in Iraq [5]. Khidher and Pilesjö [5] found that there is an anti-correlation between precipitation in Iraq and the NAO index, but also that NAO has a non-significant influence on Iraq annual temperature.

Kahya [6] found a significant relation between Turkey winter temperature/precipitation variability and NAO. The precipitation in Iran and Kuwait has a non-significant correlation with NAO, but this atmospheric mode has a significant influence on winter temperature in the western part of Iran [7,8]. In addition, the Middle East inter-annual temperature variability is related to NAO for the past century [9]. Also, the streamflow variabilities for five rivers in the Middle East (Tigris, Euphrates, Ceyhan, Karun, Yarmouk) are significantly correlated with NAO, during spring [10].

Alkhalidi et al. [11] found that the changes of ENSO circulation are warming the Indian Ocean and causing an effect on surrounding area including Iraq. In summer, the northern Shamal winds are fairly continuous from early June into July, but variations in the winds are dependent on the Indian and Arabian thermal laws [12]. Almazroui [13] found that the pressure systems that dominate on Saudi Arabian region in the summer are the Indian monsoon low, the thermal law and the subtropical high. Nasrallah et al. [14] analyzed 200 hPa maps and found that the hot, dry air masses are brought into Kuwait, Iraq and southern Turkey, due mainly to the northerly movement of the subtropical jet stream.

Kutiel et al. [15] showed that the relationship between the regional SLP and rainfall in Turkey is significant in winter and nearly non-existent during summer. Additionally, they found that above-normal SLP pressure is connected with dry conditions, while low SLP system is linked with anomalous weather conditions. Kutiel and Paz [16] found similar results in Israel: wetter conditions were associated with relatively low SLP, brought in through the Eastern Mediterranean by westerly or northerly circulation, while drier conditions were associated with relatively high SLP, and brought into the region via easterly or southerly circulation.

The Scandinavian pattern (SP), identified by Barnston and Livezey [17], is characterized in its positive phase by notable anti-cyclonic circulation over the Scandinavian region, providing rise to below-normal temperature across Western Europe and central Russia, wet condition over southern Europe, and below-normal precipitation across the Scandinavian Peninsula. Reverse conditions are typical for its negative phase [18]. Zhang [19] found that SP has an influence on the East Asian climate for respective months (September 2000–January 2001). In addition, the SP pattern affects Eurasia through winter time Rossby waves at the 500 hPa [20] using. Also, the SP influence on Eurasian climate was manifest also through Rossby wave at 300 hPa [21].

The goal of this study is to improve the understanding regarding the connection between the North Atlantic and Indian Ocean large-scale climate modes and Iraq winter and summer climate, specifically temperatures and precipitation. The introduction is followed by a short description of Iraq climate and geography. We then present data sources and methods used in this study. The results of the analyzes are presented in Section 3. The investigations are performed in two steps:

1. The SLP patterns linked to Iraq temperature and precipitation are identified through Canonical Correlation Analysis (CCA);
2. The physical mechanisms connecting these patterns with Iraq climate are inferred through regression maps.

A discussion and conclusions are included in the last two sections.

2. The Geography and Climate of Iraq

Iraq lies within the area between 29°5′ and 37°22′ N, 38° 45′ and 48°45′ E (Figure 1), in western Asia. Iraq shares borders with Turkey to the north, Iran to the east, Kuwait and Saudi Arabia to the south, Jordan to the west, and Syria to the northwest. Iraq is divided into four main geographical regions: the desert in the west, the island plateau in the middle, the northern highlands of Iraq Kurdistan, and the alluvial plain at the head of the Arabian Gulf [22].

The climate of Iraq is characterized by cool winters and hot, dry summers. Whereas in the mountain region, in northern Iraq, the climate is Mediterranean, the rest of Iraq is considered to be sub-tropical, arid to semi-arid [22,23]. During winter, the Siberian high-pressure system and sub-tropical jet stream that form over Turkey, the Arabian Peninsula and North Africa, exert a significant influence on Iraq climate. Low-pressure configurations that affect Iraq climate are the Mediterranean and Sudan systems. In summer the Indian high pressure is the most important system for Iraq climate, causing temperature increases. The associated winds are blowing north-westward [19,24].

The maximum temperature value exceeds 48 °C in summer, especially in the central and in the southern region. The winter minimum temperatures are near the freezing point in the north and around about 5 °C in the southern area [24]. Annual precipitation ranges from 100 mm to 200 mm in central and southern Iraq. In the northern region it exceeds 1000 mm/year. The majority of the annual rainfall occurs between November and April in the northern areas, and between December and February in the rest of Iraq. The rest of the year, especially from June to August, is dry [22].

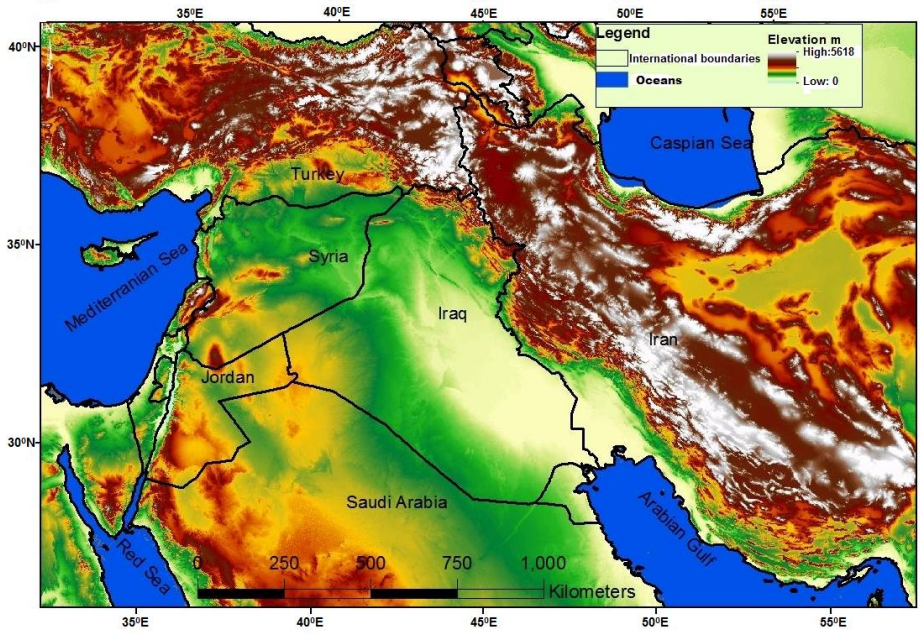

Figure 1. Regional and geographical setting of Iraq (SRTM 90 m topography map overlay by the international boundaries.

3. Data and Methodology

3.1. Data

The fields analyzed here are obtained from two data sets, European Reanalysis (ERA-Interim) and University of Delaware (UDel_AirT_PrecipV3). The first data set provided by the European Center for Medium-Range Weather Forecasts (ECMWF), for the 1979–present period [25]. The second one is provided by the Earth System Research Laboratory (ESRL), for the 1901–2010 period [26]. Both monthly data sets represent the most recent global atmospheric reanalysis data, with high quality and high homogeneity. The Iraq monthly temperatures gridded dataset are customized on a 0.25° × 0.25° resolution and with a 1° × 1° resolution for monthly SLP and GPH at 500 hPa and 200 hPa fields, for the 1979–2016 period, are obtained from ERA. On the other hand, the monthly Iraq UDel_AirT_PrecipV3 precipitation gridded dataset for the 1979–2009 period is has a 0.5° × 0.5° resolution. The relatively high resolution of temperature and precipitation fields allows investigations at the regional scale. Due to Iraq seasonality, winter and summer represent the important seasons for climate parameters. Winter and summer data anomalies are used in this study. We calculate three months averages for each season.

3.2. Methods

CCA is often used in atmospheric sciences to identify predictors or forecasters within the datasets. CCA is a multivariate statistical technique that identifies coupled patterns in two sets, with associated time series being maximum correlated [27]. Therefore, relationships between variables are highlighted through this method [28]. The vectors interrelationship may exhibit 'coupled in-phase variability' or, if

observations of the x field are made before observations of y, then the former may act as a predictor of the y field, leading to statistical forecast [27].

CCA is used in this study to identify the connections between the Iraq climate and North Atlantic/Indian Ocean atmospheric circulations. Regression maps of the GPH/SLP fields on the time series derived through CCA between the North Atlantic/Indian Ocean SLP fields and Iraq variables, were constructed in order to investigate the physical mechanisms through which the large scale patterns are connected with Iraq climate. The 95% confidence level of the statistical significance of the regression were calculated and only the significant parts of the fields are used to interpret the results of the analyzes.

4. Results

4.1. Link between the North Atlantic Region and Iraq Winter Temperature

In order to identify potential large-scale connections, a CCA was applied to winter North Atlantic SLP and Iraq temperature fields extending over the 1979–2016 period. The SLP map of the first CCA pair, explaining 32.22% of the total variance of the field, resembles the Scandinavian pattern (SP) (Figure 2a). The corresponding temperature, explaining 54.73% of the total variance, has a monopolar positive structure over Iraq area (Figure 2c). The correlation between the associated time-components is 0.76 (Figure 2b). The correlation coefficient between the SLP time component derived through CCA and the SP index is 0.35, significant at 97% confidence level according to a two-tailed test (Figure 2b). Therefore, the analysis emphasizes a link between the North Atlantic SP and Iraq winter temperature.

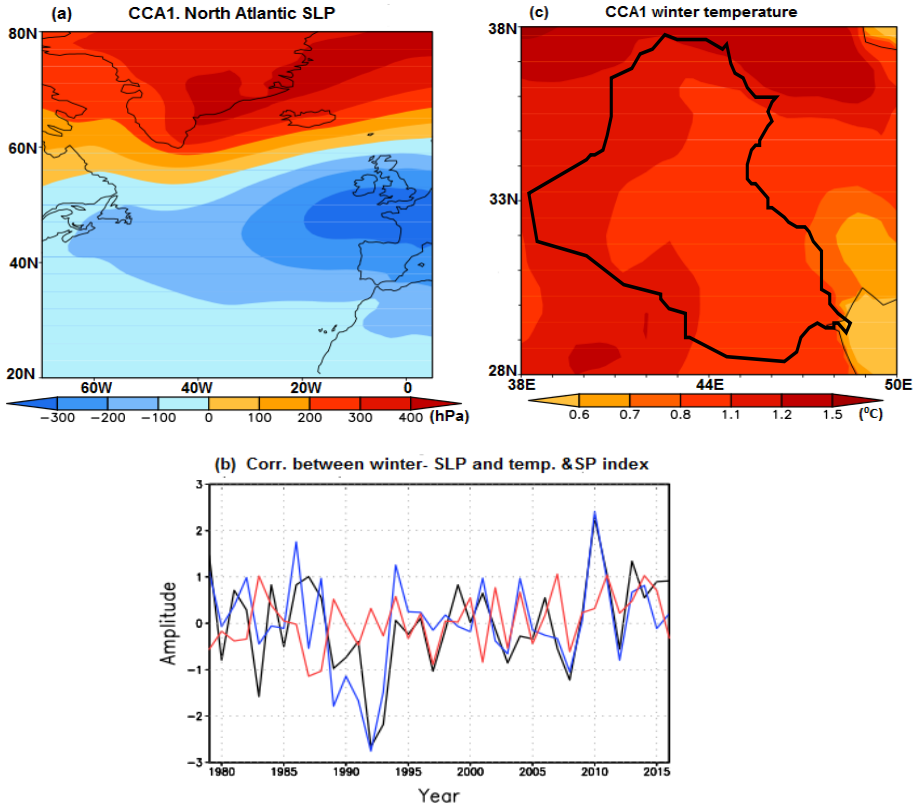

Figure 2. First pair derived through CCA between winter SLP of North Atlantic sector and Iraq winter temperature fields, extending over the 1979–2016 period. (**a**) SLP map, explaining 32.22% of the total variance; (**b**) SLP (blue line), Iraq temperature (black line) time series associated to patterns in panels (**a**,**c**), the correlation between these two time series is 0.76; (**c**) temperature map, explaining 54.73% of the total variance. The NAO index (red line in panel (**b**)) is correlated with the SLP time series at the 0.35 level. The black contour line in panel (**c**) marks the Iraq border.

4.2. Physical Processes Connecting the North Atlantic Sector with Iraq Winter Temperature

The physical mechanisms connecting the North Atlantic region with Iraq winter temperature is investigated through regression maps of the GPH 200 hPa, GPH 500 hPa and SLP on the time component associated to the SP, derived through CCA (Figure 2b), for the 1979–2016 period. The regression map of the GPH 200 hPa field on the SLP time component derived through CCA, is dominated by Rossby waves (Figure 3a), which is also visible at the 500 hPa level where it has smaller amplitude, consistent with a barotropic structure (Figure 3b). In the North Atlantic sector the SP is visible, consistent with the results derived through CCA (Figure 2a). On the surface, the SP includes a low centered over southern Europe and northern Africa. The geostrophic wind, blowing tangent to the isobars (red arrow in Figure 3c), brings warm air over Iraq and the Middle East from Africa, through northeastward advection. These conditions are consistent with the positive temperature anomalies derived through CCA (Figure 2c). In synthesis, the CCA and the regression maps, indicate that Rossby waves provide the connection between the SP and the Iraq temperature anomalies, which are locally generated by northeastward air advection from Africa.

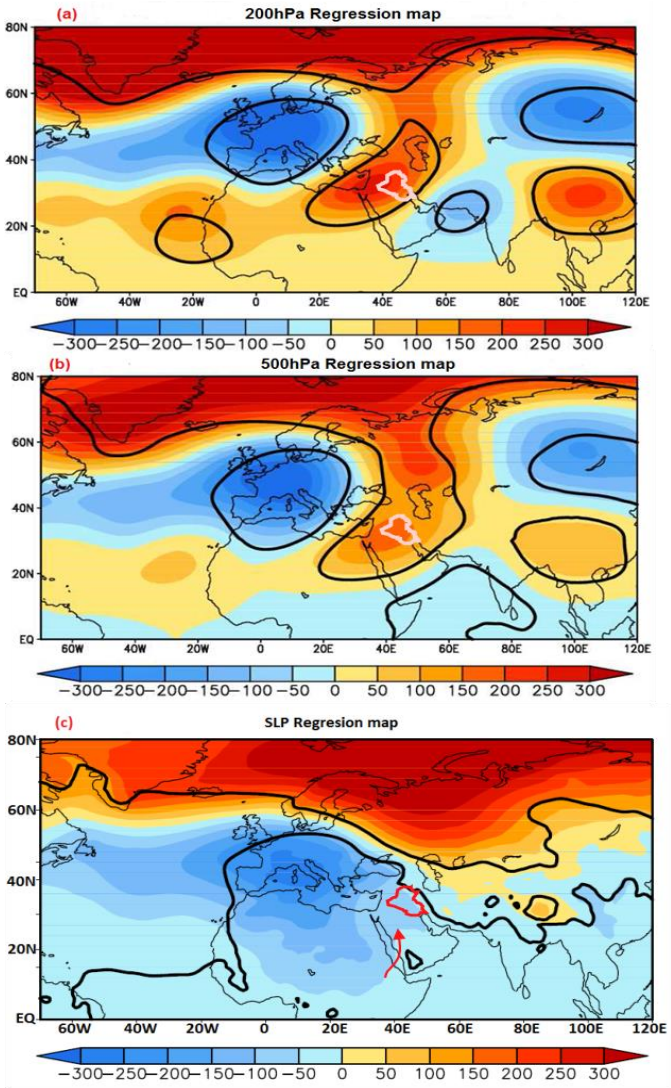

Figure 3. Regression maps of winter (**a**) geopotential height 200 hPa, (**b**) 500 hPa and (**c**) SLP fields on the time series of North Atlantic SLP associated to the first pair derived through CCA (Figure 2b), for the 1979–2016 period. The red contour lines in panels (**a**–**c**) mark the border of Iraq. The thick red arrow in panel (**c**) is used to explain the air advection. The black contour lines in panels (**a**–**c**) represent the 95% confidence level of the statistical significance of the regression.

4.3. Link between the North Atlantic Sector and Iraq Winter Precipitation

A CCA analysis was also performed in order to investigate the potential links of the North Atlantic sector with Iraq winter precipitation, for the 1979–2009 period. The SLP map of the first CCA pair, explaining 36.96% of the total variance, resembles the negative phase of NAO structure (Figure 4a). The corresponding winter precipitation map, explaining 17.71% of the total variance, has a monopolar positive structure over Iraq area, including maximum values in northeast (Figure 4c). The precipitation time-component has a significant correlation of 0.8 with the North Atlantic SLP time series (Figure 4b). The correlation coefficient between the NAO index and SLP time series derived through CCA is −0.80, significant at 99% confidence level according to two-tailed test. Therefore, the Iraq winter precipitation has a significant anti-correlation with NAO pattern.

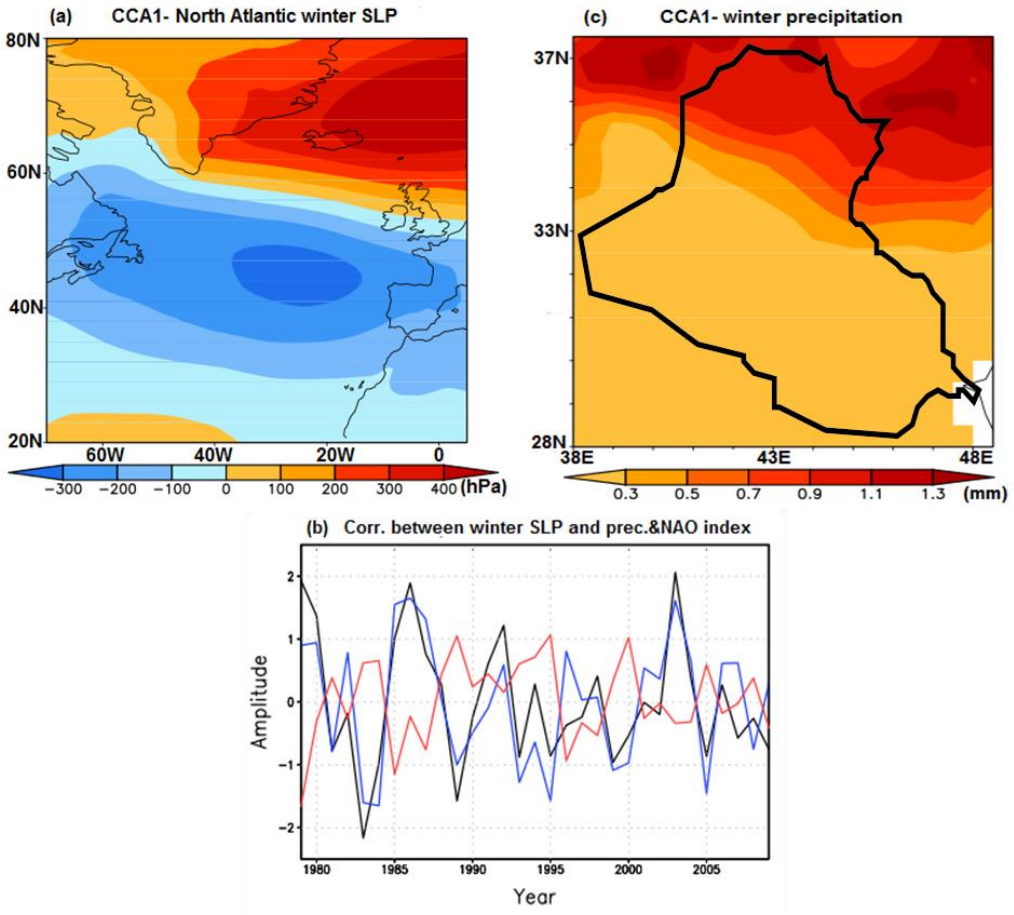

Figure 4. First pair derived through CCA between winter North Atlantic SLP and winter Iraq precipitation fields, extending over the 1979–2009 period. (**a**) SLP map, explaining 36.96% of the total variance; (**b**) SLP (blue line), Iraq precipitation (black line) time series associated to patterns in panels (**a**,**c**), the correlation between these two time series is 0.80; (**c**) precipitation map, explaining 17.71% of the total variance. The NAO index (red line in panel (**b**)) is correlated with the SLP time series at the −0.80 level. The black contour line in panel (**c**) marks the Iraq border.

4.4. Physical Processes Connecting the North Atlantic Sector with Iraq Winter Precipitation

In order to investigate the physical nature of the link between the North Atlantic Sector and Iraq winter precipitation, we constructed the regression maps of the GPH 200 hPa, GPH 500 hPa and SLP fields on the time series of SLP derived through CCA (Figure 4b), for the 1979–2009 period. The GPH 200 hPa regression map is dominated by three zonal bands with alternating signs, located

between 15° N and 80° N (Figure 5a). A very similar structure, with smaller amplitudes is observed also for the GPH 500 hPa (Figure 5b). The prominent zonal character of these two regression maps is likely related to the subtropical jet stream. At the surface, the SLP regression map is dominated by a prominent dipole centered in North Atlantic, with a low pressure system which extends toward Iraq (Figure 5c). This low could be associated with water vapor advection from North Atlantic toward middle-east. In combination with the low pressure over Iraq and associated possible local convection induced by mountains, the water vapor advection could result in positive precipitation anomalies (Figure 4c). In synthesis, the CCA and the regression maps indicate that the zonal wind and a low pressure system provide the connection between the North Atlantic sector and the Iraq precipitation anomalies, during winter.

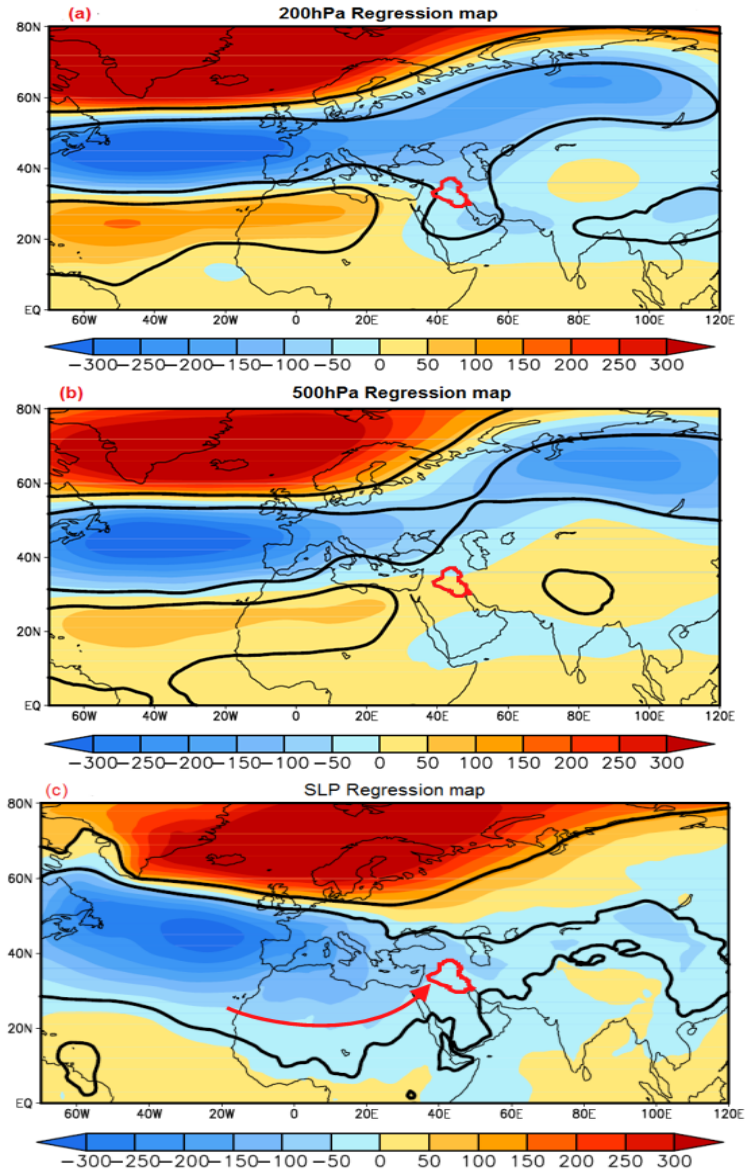

Figure 5. Regression maps of winter (**a**) geopotential height 200 hPa, (**b**) 500 hPa and (**c**) SLP fields on the time series of North Atlantic SLP associated to the first pair derived through CCA (Figure 4b), for the 1979–2009 period. The red contour lines in panels (**a**–**c**) mark the border of Iraq. The thick red arrow in panel (**c**) is used to explain the air advection. The black contour lines in panels (**a**–**c**) represent the 95% confidence level of the statistical significance of the regression.

4.5. Link between the Indian Ocean Sector and Iraq Winter Temperatures

Potential connections between the Indian Ocean SLP and Iraq winter temperature are investigated through CCA between these two fields, extending over the 1979–2016 period. The SLP map of the first CCA pair, explaining 13.13% of the total variance, is largely dominated by negative anomalies over the Indian Ocean (Figure 6a). The corresponding Iraq temperature map, explaining 62.17% of the total variance, has a positive monopolar structure over Iraq (Figure 6c). The associated time components, which show an increasing trend, are correlated at the 0.91 level (Figure 6b).

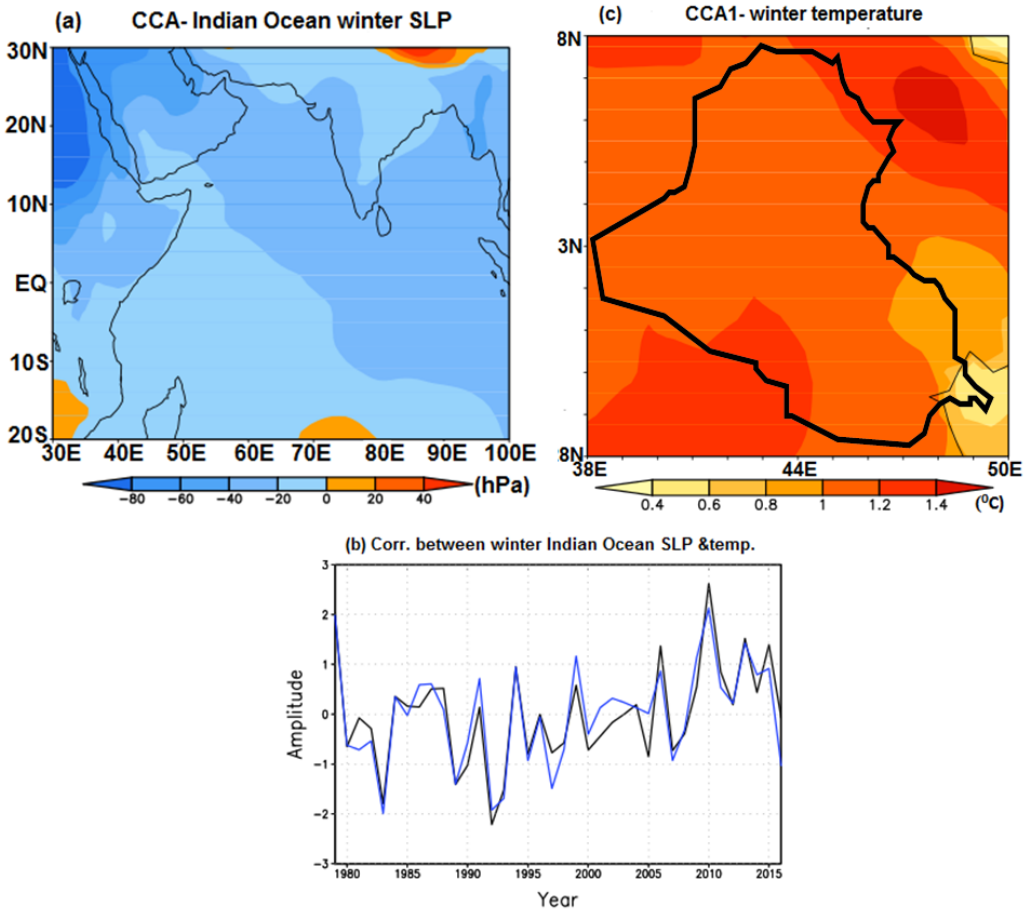

Figure 6. First pair derived through CCA between winter SLP of Indian Ocean sector and Iraq winter temperature fields, extending over the 1979–2016 period. (**a**) SLP map, explaining 13.13% of the total variance; (**b**) SLP (blue line), Iraq temperature (black line) time series associated to patterns in panels (**a**,**c**), the correlation between these two time series is 0.91; (**c**) temperature map, explaining 62.17% of the total variance. The black contour line in panel (**c**) marks the Iraq border.

4.6. Physical Mechanisms Associated with the Iraq Winter Temperature

To investigate the physical mechanisms linking the Indian Ocean sector with Iraq winter temperatures, we constructed the regression maps of the GPH 200 hPa, GPH 500 hPa and SLP fields on the time component of SLP derived through CCA (Figure 6b), for the 1979–2016 period. The GPH 200 hPa and GPH 500 hPa regression map are marked by Rossby waves, with higher amplitudes at the upper level, indicating a barotropic structure (Figure 7a,b). On the surface, the Scandinavian structure is visible (Figure 7c). Its low pressure center extending over Europe and northwest Africa brings warm over Iraq, supporting the physical consistency of the structures derived through CCA. The SLP map (Figure 7c) includes negative anomalies over Iraq, consistent with the results provided by CCA (Figure 6a). However, as mentioned above, the warm conditions over Iraq appear to be generated by

the low pressure system centered over Europe, with no significant contribution from the Indian Ocean sector. Therefore, although the Indian Ocean SLP anomalies are correlated with Iraq temperature, as shown by the CCA, the regression maps indicate that the low pressure system included in the Scandinavian pattern has a significant connection with Iraq winter temperature. Rossby waves provide the link between the North Atlantic sector and Iraq climate.

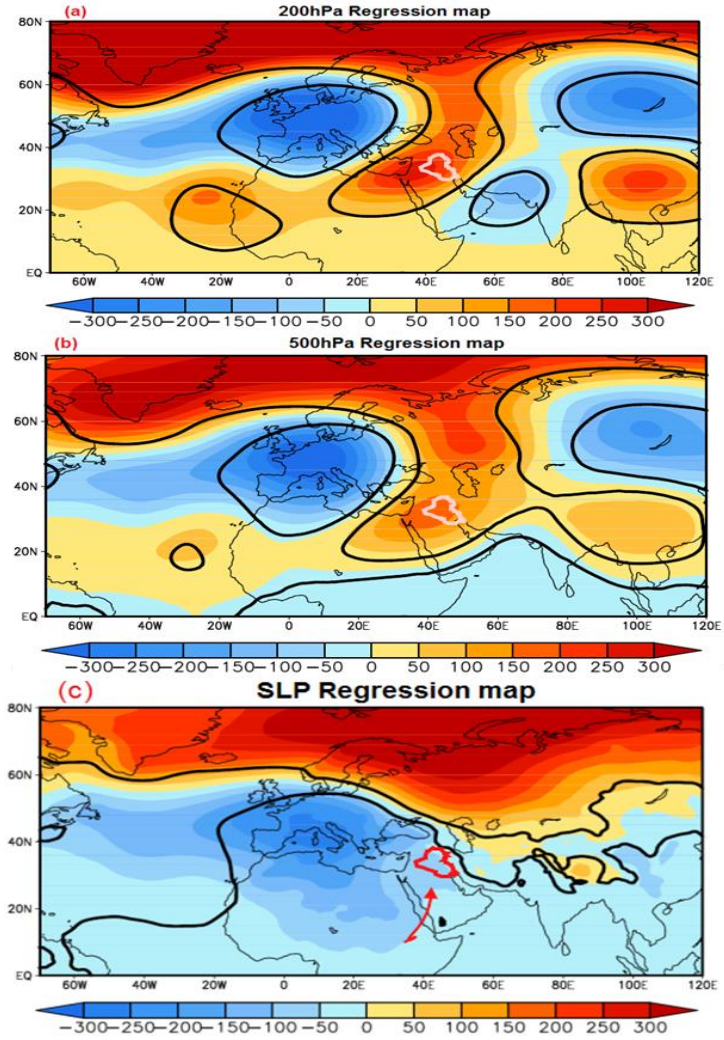

Figure 7. Regression maps of winter (**a**) geopotential height 200 hPa, (**b**) 500 hPa and (**c**) SLP fields on the time series of Indian Ocean SLP associated to the first pair derived through CCA (Figure 6b), for the 1979–2016 period. The red contour lines in panels (**a**–**c**) mark the border of Iraq. The thick red arrow in panel (**c**) is used to explain the air advection. The black contour lines in panels (**a**–**c**) represent the 95% confidence level of the statistical significance of the regression.

4.7. Link between the Indian Ocean Sector and Iraq Summer Temperature

A CCA was performed also for the summer seasons, in order to identify potential links between Iraq temperature and the Indian Ocean SLP during this season, for the 1979–2016 period. The SLP map of the first CCA pair, explaining 7.73% of the total variance, includes a maximum over India and minimum over the Arab Peninsula (Figure 8a). The corresponding summer temperature has a positive monopolar structure over Iraq area (Figure 8c) and explains 66.31% of the total variance. The associated time components are marked by a prominent shift to positive values, located around 1998. The correlation between the two time series is 0.88 (Figure 8b). A similar CCA between North Atlantic SLP and Iraq summer temperature and precipitation indicates non-significant connection

between these two sectors for this season, also, non-considerable links between Iraq winter/summer precipitation and Indian Ocean SLP are investigated (not shown).

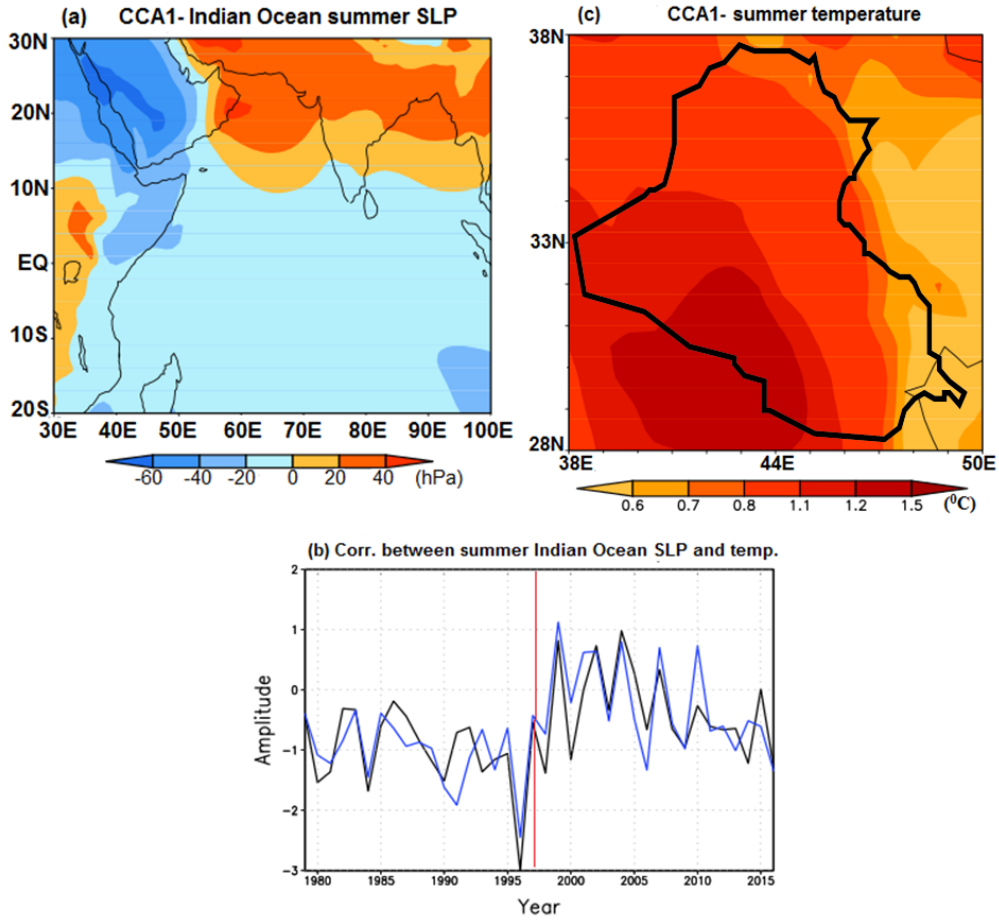

Figure 8. First pair derived through CCA between summer SLP of Indian Ocean sector and Iraq summer temperature fields extending over the 1979–2016 period. (**a**) SLP map, explaining 7.73% of the total variance; (**b**) SLP (blue line), Iraq temperature (black line) time series associated to patterns in panels (**a**,**c**), the correlation between these two time series is 0.88; (**c**) temperature map, explaining 66.31% of the total variance. The black contour line in panel (**c**) marks the Iraq border.

4.8. Physical Mechanisms Associated to Iraq Summer Temperature

The physical mechanisms connecting the Indian Ocean sector with Iraq summer temperatures was investigated through regression maps of the GPH 200 hPa, GPH 500 hPa and SLP fields on the time series of SLP, derived through CCA (Figure 8b). The GPH 200 hPa and GPH 500 hPa regression maps include a barotropic Rossby wave-like structure, with a higher wave number that that derived for the winter season (Figure 9a,b). At the surface (Figure 9c), a significant gradient pressure gradient is located over Iraq and extends toward the Indian Ocean, consistent with the CCA (Figure 8a). The associated circulation brings the hot air from the India and Africa through Arabian Desert to Iraq, consistent with the positive temperature anomalies derived through CCA (Figure 8c). In synthesis, the Iraq summer temperature is connected to the warm air advection from the India and Africa through Arabia Peninsula.

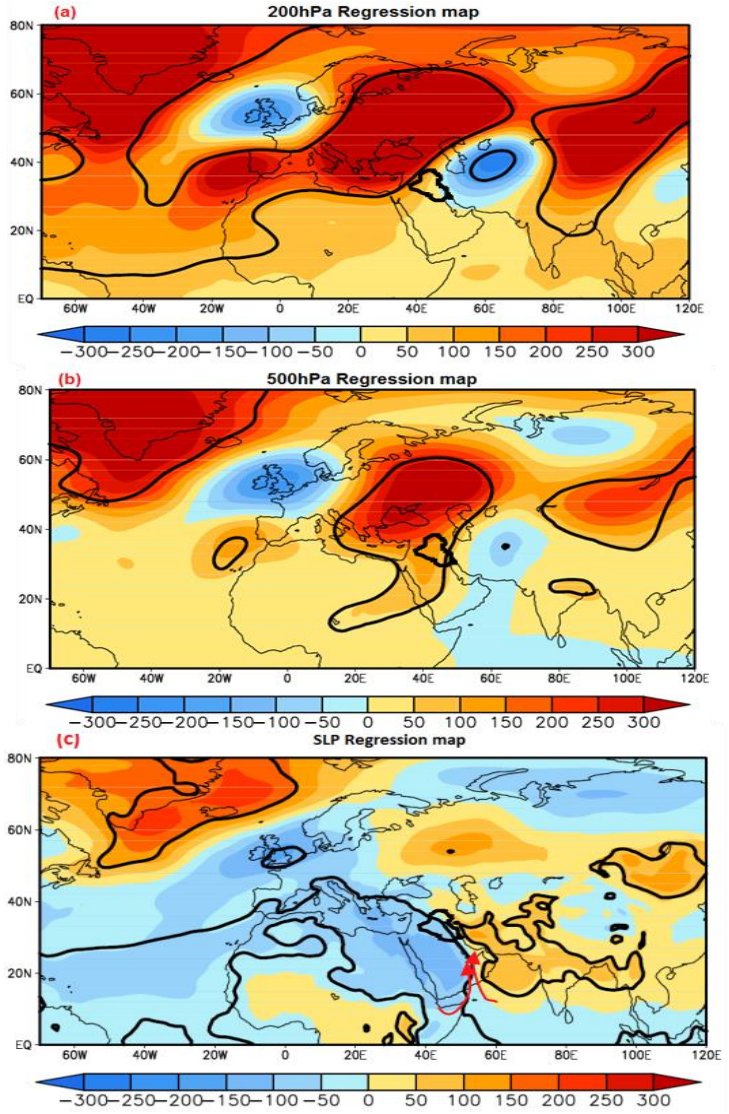

Figure 9. Regression maps of summer (**a**) geopotential height 200 hPa, (**b**) 500 hPa and (**c**) SLP fields on the time series of Indian Ocean SLP associated to the first pair derived through CCA (Figure 8b), for the 1979–2016 period. The red contour lines in panels (**a**,**c**) mark the border of Iraq. The thick red arrows in panel (**c**) are used to explain the air advection. The black contour lines in panels (**a**,**c**) represent the 95% confidence level of the statistical significance of the regression.

The possible asymmetries of the connections identified here in respect with the sign of Iraq climate anomalies were investigate through composite maps (not shown). All features described above have a symmetric character.

5. Discussion

In this study, we investigated the links between the North Atlantic and Indian Ocean sectors and Iraq climate during winter and summer. The North Atlantic SP has a significant correlation with Iraq winter temperatures. Rossby waves are connecting the two sectors through the free atmosphere. At Earth's surface, the air advection from Africa via the northeastward wind appears to be the main mechanism linking the North Atlantic sector with the Iraq temperature. Additionally, the similar studies indicate that the Middle-East inter-annual temperature variability is related to atmospheric modes associated with NAO [9], Khidher and Pilesjo [5] found that Iraq winter temperatures were influenced by stable patterns over North Atlantic area, rather than by the NAO. In addition,

Bueh and Nakamura [21] investigate the link between the SP and Eurasian climate through the dynamical properties, including Rossby wave's structure at 300 hPa. For summer, Nasrallah et al. [14] investigate found that the movement of the Arabian Desert hot dry air mass over the northeastern Arabian Peninsula, Kuwait, the northern Arabian Gulf and southern Iraq, generates a rise of the surface temperature.

Iraq winter precipitations are linked to the NAO pattern. The advection of wet air associated with low-pressure conditions, from the North Atlantic toward Iraq, through North Africa, causes precipitation anomalies in this country. The results are consistent with the finding of Khidher and Pilesjo [5] that the NAO has a significant anti-correlation with Iraq precipitation, through the cyclones that are formed over the Mediterranean Sea and migrate toward this area. Furthermore, the finding of Alpert et al. [29] that the Sharav cyclone along the north Africa coast represents an important cold front influencing the southeastern Mediterranean through the jet stream. Also, Trigo et al. [30] found that northern Mediterranean region climate is influenced indirectly by the change in North Atlantic climate and directly by local severe storm. In addition, the variabilities of streamflows of five revers from the Middle East (Tigris, Euphrates, Ceyhan, Karun, and Yarmok) are significantly correlation with the NAO index [10].

Iraq summer temperature is connected to the pressure gradient over the Arabian Desert and India. Similar studies, such as of Nasrallah et al. [14] and Khidher [24] found that Iraq summer climate is influenced by the Indian high-pressure system, which increases the temperature over the Arabian Desert, Iraq and the southern part of Turkey. Additionally, the study of Kampf and Sandrinasab [12] found that the variations in the winds over Arabian Peninsula depended on the Indian and Arabian thermal laws in summer. Also, Almazroui [13] found that the pressure systems that dominate the Arabian Desert are the subtropical high and thermal law, in summer.

6. Conclusions

The results presented here provide a new perspective on the connections between North Atlantic and Indian Ocean sectors and Iraq temperature and precipitation, during boreal winter and summer. The associated physical mechanisms are also investigated through regression maps. The main conclusions of this study are summarized below.

The Iraq winter temperature anomalies are linked to SP, reflecting a North Atlantic influence over Iraq climate, as part of Rossby waves, which provide the connections between the two sectors. Locally, the Iraq anomalies appear to be generated by air advection from Africa (Figures 2 and 3). Iraq winter precipitations are linked with the North Atlantic Oscillation mainly through zonal atmospheric circulation, with air advection playing and important role at the surface (Figures 4 and 5). During winter, the Iraq temperature and precipitations are connected mainly by processes linked to the North Atlantic, with un-significant connection to the Indian Ocean sector (Figures 6 and 7). Iraq summer temperature is linked to a pressure gradient located in the Middle East, which intensified significantly around 1998 (Figures 8 and 9). In synthesis, our study indicates that the dominant modes of Iraq temperature and precipitation variability are largely linked to continental scale atmospheric structures largely connected to the North Atlantic sector, with less link from the Indian Ocean.

Acknowledgments: We highly appreciate the ECMWF and ESRL for providing the data. The first author would like to thank the Iraq ministry of higher education and scientific research for support.

Author Contributions: J.A. and M.D. conceived and designed the experiments; J.A. wrote the paper, performed the experiments and analyzed the data; M.D. contributed to manuscript improvement and revisions; P.V. contributed analysis tools; S.S. modified the manuscript.

Conflicts of Interest: The authors declare no conflict of interest.

References

1. Hurrell, J.W. Decadal trends in the North Atlantic Oscillation: Regional temperatures and precipitation. *Sci. New Ser.* **1995**, *269*, 676–679. [CrossRef] [PubMed]
2. Scaife, A.A.; Folland, C.K.; Alexander, L.V.; Moberg, A.; Knight, J.R. European climate extremes and the North Atlantic Oscillation. *J. Clim. Am. Meteorol. Soc.* **2008**, *21*, 72–83. [CrossRef]
3. Dima, M.; Rimbu, N.; Stefan, S.; Dima, I. Quasi-Decadal Variability in the Atlantic Basin Involving Tropics-Midlatitudes and Ocean-Atmosphere Interactions. *J. Clim.* **2001**, *14*, 823–832. [CrossRef]
4. Muñoz, D.; Rodrigo, F.S. Impacts of the North Atlantic Oscillation on the probability of dry and wet winters in Spain. *Clim. Res.* **2004**, *4*, 33–43. [CrossRef]
5. Khidher, S.A.; Pilesjö, P. The effect of the North Atlantic Oscillation on the Iraqi climate 1982–2000. *Theor. Appl. Climatol.* **2015**, *122*, 771. [CrossRef]
6. Kahya, E. The Impacts of NAO on the Hydrology of the Eastern Mediterranean (Chapter 4). *Adv. Glob. Chang. Res.* **2011**, *46*, 51–71.
7. Masih, I.; Uhlenbrook, S.; Maskey, S.; Smakhtin, V. Streamflow trends and climate linkages in the Zagros Mountains, Iran. *Clim. Chang.* **2010**, *104*, 317–338. [CrossRef]
8. Marcella, M.P.; Eltahir, E. The hydroclimatology of Kuwait: Explaining the variability of rainfall at seasonal and interannual time scales. *J. Hydrometeorol.* **2008**, *9*, 1095–1105. [CrossRef]
9. Mann, M.E. Large-scale climate variability and connections with the middle-east in the past Centuries. *Clim. Chang.* **2002**, *55*, 278–314. [CrossRef]
10. Cullen, H.M.; Demenocal, P. North Atlantic influence on Tigris-Euphrates streamflow. *Int. J. Climatol.* **2000**, *55*, 853–863. [CrossRef]
11. Alkhalidi, J.; Dima, M.; Stefan, S. Large-scale modes impact on Iraq climate variability. *Theor. Appl. Climatol.* **2017**, *129*, 1–12. [CrossRef]
12. Kampf, J.; Sadrinasab, M. The circulation of the Persian Gulf: A numerical study. *Ocean Sci.* **2006**, *2*, 27–41. [CrossRef]
13. Almazroui, M.A.; Al Khalaf, A.K.; Abdel Basset, H.M.; Hasanean, H.M. *Detecting Climate Change Signals in Saudi Arabia Using Surface Temperature*; Project Number (305/428); King Abdelaziz University: Kingdom of Saudi Arabia, 2009.
14. Nasrallah, H.A.; Nieplova, E.; Ramadan, E. Warm season extreme temperature events in Kuwait. *J. Arid Environ.* **2004**, *56*, 357–371. [CrossRef]
15. Kutiel, H.; Hirsch, T.R.; Turkes, M. Sea level pressure patterns associated with dry or wet monthly rainfall conditions in Turkey. *Theor. Appl. Climatol.* **2001**, *69*, 39–67. [CrossRef]
16. Kutiel, H.; Paz, S. Sea Level Pressure Departures in the Mediterranean and their Relationship with Monthly Rainfall Conditions in Israel. *Theor. Appl. Climatol.* **1998**, *60*, 93–109. [CrossRef]
17. Barnston, A.G.; Livezey, R.E. Classification, seasonality and persistence of low-frequency atmospheric circulation patterns. *Mon. Weather Rev.* **1987**, *115*, 1083–1126. [CrossRef]
18. CPC. Northern Hemisphere Teleconnection Patterns. 2005. Available online: www.cpc.noaa.gov/data/teleconents.shtml (accessed on 1 March 2017).
19. Zhang, J. January 2001—Low temperature in the northeastern China and heavy snowstorm over Inner Mongolia and Xinjiang. *Mon. Meteorol.* **2001**, *27*, 62–63. (In Chinese)
20. Ohhashi, Y.; Yamazaki, K. Variability of the Eurasian pattern and its interpretation by wave activity flux. *J. Meteorol. Soc. Jpn.* **1999**, *77*, 495–511. [CrossRef]
21. Bueh, C.; Nakamura, H. Scandinavian pattern and its climatic impact. *Q. J. R. Meteorol. Soc.* **2007**, *133*, 2117–2131. [CrossRef]
22. Frenken, K. *Irrigation in the Middle East Region in Figures—AQUASTAT Survey 2008*; FAO: Rome, Italy, 2009.
23. Khamis, M.D. Identifying the climatic conditions in Iraq by tracking down cooling events in the North Atlantic Ocean in the period 3000–BC. *Misc. Geogr.* **2014**, *18*, 40–46.
24. Khidher, S.A. *Climate History of Iraq, Past and Present*; (Book in Arabic); Baghdad University Press: Baghdad, Iraq, 2013.
25. Dee, D.P.; Uppala, S.M.; Simmons, A.J. The ERA-Interim reanalysis: Configuration and performance of the data assimilation system. *Q. J. R. Meteorol. Soc.* **2011**, *137*, 553–597. [CrossRef]

26. Willmott, C.J.; Matsuura, K. Terrestrial Air Temperature and Precipitation: Monthly and Annual Time Series (1950–1999). 2001. Available online: https://www.esrl.noaa.gov/psd/data (accessed on 1 April 2017).
27. Wilks, D.S. *Statistical Methods in the Atmospheric Sciences*, 3rd ed.; Academic Press: Oxford, UK, 2011; Volume 100.
28. Marzban, C.; Sandgathe, S.; Doyle, J.D. Model Tuning with Canonical Correlation Analysis. *Mon. Weather Rev.* **2014**, *142*, 2018–2027. [CrossRef]
29. Alpert, P.; Ziv, B. The Sharav cyclone: Observations and some theoretical considerations. *J. Geophys. Res.* **1989**, *94*, 18495–18514. [CrossRef]
30. Trigo, I.F.; Davis, T.D.; Bigg, G.R. Decline in Mediterranean rainfall caused by weakening of Mediterranean cyclones. *Geophys. Res. Lett.* **2000**, *27*, 2913–2916. [CrossRef]

© 2017 by the authors. Licensee MDPI, Basel, Switzerland. This article is an open access article distributed under the terms and conditions of the Creative Commons Attribution (CC BY) license (http://creativecommons.org/licenses/by/4.0/).